

Optically Transparent Sulfur-Containing Polyimide–TiO₂ Nanocomposite Films with High Refractive Index and Negative Pattern Formation from Poly(amic acid)–TiO₂ Nanocomposite Film

Jin-gang Liu, Yasuhiro Nakamura, Tomohito Ogura, Yuji Shibasaki, Shinji Ando, and Mitsuru Ueda*

Department of Organic and Polymeric Materials, Tokyo Institute of Technology, 2-12-1-H120 O-okayama, Meguro-ku, Tokyo 152-8552, Japan

Received May 25, 2007. Revised Manuscript Received October 26, 2007

A series of semialicyclic polyimides (PIs) have been successfully prepared by the polycondensation of two alicyclic dianhydrides, 1,2,3,4-cyclobutanetetracarboxylic dianhydride (CBDA) and 1,2,4,5-cyclohexanetetracarboxylic dianhydride (CHDA) with two sulfur-containing aromatic diamines, 4,4'-thiobis[*p*-phenylenesulfanyl]aniline] (3SDA) and 2,7-bis(4-aminophenylenesulfanyl)thianthrene (APTT), respectively, by a two-step polymerization procedure via the soluble poly(amic acid) (PAA) precursors. Flexible and tough PI films were obtained with a tensile strength greater than 82 MPa and elongation at breaks higher than 12%. The films showed good thermal and thermal-oxidative stability without significant weight loss up to 400 °C, both in air and nitrogen. The glass-transition temperatures of the PIs ranged from 236.5 to 274.1 °C. Good optical transparency, including the cutoff wavelengths lower than 350 nm and transmittances higher than 80% at 400 nm, was achieved for all the PI films. The refractive indices of the PI films were in the range of 1.6799–1.7130 measured at 632.8 nm, which agreed well with the values calculated by the time-dependent density functional theory (TD-DFT). In addition, PAA-II_a (CHDA-3SDA) showed a good affinity with silica-modified TiO₂ nanoparticles. The hybrid system with 45 wt % load of TiO₂ nanoparticles, combined with the photobase generator *N*-{[(4,5-dimethoxy-2-nitrobenzyl)oxy]carbonyl}2,6-dimethylpiperidine (DNCDP) exhibited good photolithographic characteristics. A fine negative pattern with a resolution of approximately 4 μm was successfully printed on the hybrid film. The cured PI-II_a–TiO₂ hybrid film exhibited a refractive index of 1.8100 at 632.8 nm.

Introduction

High refractive index (high-*n*) and low birefringence (Δn) combined with good thermal stability and high optical transparency are the basic concerns in designing optical polymer coatings for high-performance CMOS image sensors (CIS).^{1–3} Conventional high-*n* optical polymers such as sulfur-containing epoxy,⁴ poly(methyl methacrylate) (PMMA),⁵ and polyurethane⁶ can meet most of the requirements. However, the relatively poor thermal stability of the polymers often limits their wide applications. Furthermore, the conventional high-*n* polymers usually exhibit refractive indices of 1.6–1.7, which are not high enough for CIS applications ($n > 1.8$).⁷ Wholly aromatic polyimides (PIs), a well-known class of thermal-resistant polymers, have been increasingly

applied in advanced optical fabrications after several decades of scientific and technical evaluations.^{8–12} PIs possess good combined properties, including high thermal and radiation stability, high mechanical and dielectric properties, and in particular, inherent high refractive index; hence, they are considered as one of the best candidates as high-*n* polymers.¹³ For example, the PI derived from bis[4-(3,4-dicarboxyphenoxy) phenyl]propane dianhydride (BPADA) and 4,4'-oxidianiline (ODA) showed a refractive index of 1.66 at 632.8 nm as well as a low birefringence.¹⁴

Although the conventional PIs exhibited considerably higher refractive indices than those of the common optical polymers, their poor transparency in the visible light region, caused by the formation of charge-transfer complexes (CTC) between the electron-donating diamine moiety and the electron-accepting dianhydride moiety, might be a serious

* To whom correspondence should be addressed. Tel: 81-3-57342127. Fax: 81-3-57342127. E-mail: ueda.m.ad@m.titech.ac.jp.

- (1) Regolini, J. L.; Benoit, D.; Morin, P. *Microelectron. Reliab.* **2007**, *47*, 739.
- (2) Cox, C.; Planjec, C.; Brakensiek, N.; Zhu, Z. M.; Mayo, J. *Proc. SPIE* **2006**, *6153*, 61534E.
- (3) Nakai J.; Aoki T. US Patent 7087945, **2006**.
- (4) Lu, C. L.; Cui, Z. C.; Wang, Y. X.; Yang, B.; Shen, J. C. *J. Appl. Polym. Sci.* **2003**, *89*, 2426.
- (5) Minns, R. A.; Gaudiana, R. A. *J. Macromol. Sci., Pure Appl. Chem.* **1992**, *A29*, 19.
- (6) Lu, C. L.; Cui, Z. C.; Wang, Y.; Li, Z.; Guan, C.; Yang, B.; Shen, J. C. *J. Mater. Chem.* **2003**, *13*, 2189.
- (7) Suwa, M.; Niwa, H.; Tomikawa, M. *J. Photopolym. Sci. Technol.* **2006**, *19*, 275.

- (8) Watanabe, Y.; Shibasaki, Y.; Ando, S.; Ueda, M. *Chem. Mater.* **2002**, *14*, 1762.
- (9) Watanabe, Y.; Shibasaki, Y.; Ando, S.; Ueda, M. *Polym. J.* **2006**, *38*, 79.
- (10) (a) Ma, H.; Jen, A. K. Y.; Dalton, L. R. *Adv. Mater.* **2002**, *14*, (b) Tsuda, Y.; Yoshida, T.; Kakoi, T. *Polym. J.* **2006**, *38*, 88.
- (11) Sakayori, K.; Shibasaki, Y.; Ueda, M. *Polym. J.* **2006**, *38*, 1189.
- (12) Ogura, T.; Yamaguchi, K.; Shibasaki, Y.; Ueda, M. *Polym. J.* **2007**, *39*, 245.
- (13) Flaim, T.; Wang, Y. B.; Mercado, R. *Proc. SPIE* **2004**, *5250*, 423.
- (14) Eichstadt, A. E.; Ward, T. C.; Bagwell, M. D.; Farr, I. V.; Dunson, D. L.; McGrath, J. E. *Macromolecules* **2002**, *35*, 7561.

obstacle to their wide applications.¹⁵ Considerable efforts have been made to modify the coloration of the conventional PIs. However, according to the Lorentz–Lorenz equation,¹⁶ most of the procedures that aim to decrease the polarizability of the PI molecular chains, such as the introduction of electron-withdrawing fluoro atoms or fluoro-containing substituents,^{17–19} the incorporation of alicyclic moieties,²⁰ and the modification of the molecular skeleton by meta-substituted structures,²¹ often decrease the refractive indices of the PIs. Thus, it is an interesting and challenging project to develop high-*n* PIs with high transparency.

Recently, with the rapid development of nanoscience and technology, an effective method for developing high-*n* polymers has been revealed, i.e., to combine the high-*n* inorganic nanoparticles such as TiO₂ (anatase, *n* = 2.45; rutile, *n* = 2.70),²² ZrO₂ (*n* = 2.10),²³ amorphous silicon (*n* = 4.23), PbS (*n* = 4.20),²⁴ or ZnS (*n* = 2.36)²⁵ with an organic polymer matrix in order to develop an organic–inorganic nanocomposite system. When the sizes of the high-*n* nanoparticles are below 50 nm, the nanocomposite films are often optically transparent.^{26,27} In addition, the refractive indices of the nanocomposites can be approximately estimated by the equation of $n_{\text{comp}} = \varphi_p n_p + \varphi_{\text{org}} n_{\text{org}}$,^{27,28} where n_{comp} , n_p , and n_{org} are the refractive indices of the nanocomposite, nanoparticle, and organic matrix, respectively. φ_p and φ_{org} are the volume fractions of the nanoparticles and organic matrix, respectively. Thus, it can be concluded from the equation that to achieve a definite n_{comp} value with a definite type of nanoparticle, the higher the value of n_{org} , the lower the value of φ_p . This is important for the design of high-*n* nanocomposites for optical applications because an overload of the nanoparticles often increases the optical loss and decreases the processability of the organic matrix.²⁹

Our previous works on high-*n* PIs revealed that the incorporation of thioether-containing moieties could effectively increase the refractive indices and decrease the birefringences of the PIs.^{30–32} However, the optical transpar-

ency of the sulfur-containing PI films in the visible light region is not sufficiently high and should be improved.

In this study, we report a photoimagable and optically transparent sulfur-containing semialicyclic polyimide–TiO₂ nanocomposite film with a high refractive index. The semialicyclic polyimides were prepared from the alicyclic dianhydrides, 1,2,3,4-cyclobutanetetracarboxylic dianhydride (CBDA) and 1,2,4,5-cyclohexanetetracarboxylic dianhydride (CHDA), and the thioether-linked aromatic diamines, 4,4'-thiobis[*p*-(phenylenesulfanyl)aniline] (3SDA) and 2,7-bis(4-aminophenylenesulfanyl)thianthrene (APTT), by a two-step polymerization procedure via the soluble poly(amic acid) (PAA) precursors. The semialicyclic PIs exhibited high refractive indices in the range of 1.6799–1.7130 with high thermal stability (>400 °C), high transparency (>400 nm), and low birefringence in the range of 0.0048–0.0220. The semialicyclic PAA-II_a derived from CHDA and 3SDA exhibited high compatibility with the silica-modified TiO₂ nanoparticle, thereby resulting in a highly transparent PI film at 365 nm with a high refractive index of 1.8100 at 632.8 nm. The photolithographic property of the PAA-II_a–TiO₂ hybrid system was also investigated.

Experimental Section

Materials. 1,2,3,4-Cyclobutanetetracarboxylic dianhydride (CBDA, Japan Synthetic Rubber Co., Ltd.) and 1,2,4,5-cyclohexanetetracarboxylic dianhydride (CHDA, or hydrogenated pyromellitic dianhydride, HPMDA, New Japan Chemical Co., Ltd.) were kindly supplied by the companies and dried in vacuo at 120 °C for 24 h prior to use. 4,4'-Thiobis[*p*-(phenylenesulfanyl)aniline] (3SDA) and 2,7-bis(4-aminophenylenesulfanyl)thianthrene (APTT) were synthesized in-house according to the methods described in our previous studies.^{31,32} The photobase generator *N*-{[(4,5-dimethoxy-2-nitrobenzyl)-oxy]carbonyl}–2,6-dimethylpiperidine (DNCDP) was synthesized according to the literature.³³ Silica-modified anatase-type TiO₂ nanoparticles with diameters of 10 nm were purchased from Catalysts & Chemicals Ind. Co., Ltd., Japan (*n* = 2.0 at 589 nm; *d* = 3.11 g/cm³), and used as received. Tetramethylammonium hydroxide (TMAH) aqueous solution (15 wt %) was purchased from Wako, Japan, and diluted to 2.38 wt % with deionized water before use. *N*-Methyl-2-pyrrolidinone (NMP) for the PI synthesis was purchased from Wako, Japan, and distilled over CaH₂ in vacuo and stored over 4 Å molecular sieves.

Characterization. The inherent viscosity was measured using an Ubbelohde viscometer with a 0.5 g/dL NMP solution at 30 °C. The Fourier transform infrared (FT-IR) spectra were obtained using a Horiba model FT-120 Fourier transform-IR spectrophotometer. The ultraviolet–visible (UV–vis) spectra were recorded on a Hitachi U-3210 spectrophotometer at room temperature. The PI films were dried at 100 °C for 1 h before testing to remove the absorbed moisture. Wide-angle X-ray diffraction was conducted on a Rigaku D/max-2500 X-ray diffractometer with Cu Kα1 radiation, operated at 40 kV and 200 mA. Thermogravimetric analysis (TGA) was performed using a Seiko TG/DTA 6300 thermal analysis system at a heating rate of 10 °C/min in a flow of nitrogen or air (200 mL/min). Differential scanning calorimetry (DSC) was performed

- (15) Ando, S.; Matsuura, T.; Sasaki, S. *Polym. J.* **1997**, *29*, 69.
- (16) Matsuda, T.; Funae, Y.; Yoshida, M.; Takaya, T. *J. Macromol. Sci., Pure Appl. Chem.* **1999**, *A36*, 1271.
- (17) Yang, C. P.; Su, Y. Y.; Hsu, M. Y. *Polym. J.* **2006**, *38*, 132.
- (18) Yang, C. P.; Chen, Y. P.; Woo, E. M.; Li, S. H. *Polym. J.* **2006**, *38*, 457.
- (19) Carter, K. R.; Dipietro, R. A.; Sanchez, M. I.; Swanson, S. A. *Chem. Mater.* **2001**, *13*, 213.
- (20) Tsuda, Y.; Kuwahara, R.; Fukuda, K.; Ueno, K.; Oh, J. M. *Polym. J.* **2005**, *37*, 126.
- (21) Clair, K.; Clair, T. L.; Winfree, W. P. *Proc. Am. Chem. Soc., Div. Polym. Mater. Sci. Eng.* **1988**, *59*, 28.
- (22) Yuwono, A. H.; Liu, B. H.; Xue, J. M.; Wang, J.; Elim, H. I.; Ji, W.; Li, Y.; White, T. J. *J. Mater. Chem.* **2004**, *14*, 2978.
- (23) Suzuki, N.; Tomita, Y.; Ohmori, K.; Hidaka, M.; Chikama, K. *Opt. Express* **2006**, *14*, 12712.
- (24) Papadimitrakopoulos, F.; Wisniecki, P.; Bhagwagar, D. E. *Chem. Mater.* **1997**, *9*, 2928.
- (25) Lu, C. L.; Cui, Z. C.; Li, Z.; Yang, B.; Shen, J. C. *J. Mater. Chem.* **2003**, *13*, 526.
- (26) Zimmermann, L.; Weibel, M.; Caseri, W.; Suter, U. W.; Walther, P. *Polym. Adv. Technol.* **1993**, *4*, 1.
- (27) Weibel, M.; Caseri, W.; Suter, U. W.; Kiess, H.; Wehrli, E. *Polym. Adv. Technol.* **1991**, *2*, 1.
- (28) Althues, H.; Henle, J.; Kaskel, S. *Chem. Soc. Rev.* **2007**, *9*, 1454.
- (29) Paquet, C.; Cyr, P. W.; Kumacheva, E.; Manners, I. *Chem. Commun.* **2004**, 234.
- (30) Liu, J. G.; Nakamura, Y.; Shibasaki, Y.; Ando, S.; Ueda, M. *Polym. J.* **2007**, *39*, 543.

- (31) Liu, J. G.; Nakamura, Y.; Shibasaki, Y.; Ando, S.; Ueda, M. *J. Polym. Sci., Part A: Polym. Chem.* **2007**, *45*, 5606.
- (32) Liu, J. G.; Nakamura, Y.; Shibasaki, Y.; Ando, S.; Ueda, M. *Macromolecules* **2007**, *40*, 4614.
- (33) Mochizuki, A.; Teranishi, T.; Ueda, M. *Macromolecules* **1995**, *28*, 365.

on a Seiko 6300 at a heating rate of 10 °C/min. Dynamic mechanical thermal analysis (DMA) was performed on the PI film specimens (30 mm long, 10 mm wide, and 50–60 μm thick) on a Seiko DMS 6300 at a heating rate of 2 °C/min with a load frequency of 1 Hz in air. The glass-transition temperature (T_g) was determined as the peak temperature in the loss-modulus (E'') plot. The mechanical properties were measured on a Toyo Baldwin Tensilon/UTM-11–20 tester with a load cell of 20 kg at a drawing speed of 4 mm/min. Measurements were performed on five PI film specimens (30 mm × 10 mm × 0.080 mm) at room temperature, and the corresponding results were determined as the average values of the five parallel determinations. The film thickness was measured on a Dektak³ surface profiler system from Veeco Instruments Inc. Field-emission scanning electron microscopy (SEM) was carried out using a Technex Laboratory Tiny-SEM 1540 with an accelerating voltage of 15 KV for imaging. Pt/Pd was sputtered on each film in advance of the SEM measurements.

The in-plane (n_{TE}) and out-of-plane (n_{TM}) refractive indices of PI films whose thicknesses are more than 3 μm were measured using a prism coupler (Metricon, model PC-2000) equipped with a He–Ne laser light source (wavelength: 632.8 nm). The in-plane (n_{TE})/out-of-plane (n_{TM}) birefringence (Δn) was calculated as the difference between n_{TE} and n_{TM} . The average refractive index (n_{av}) was calculated using eq 1

$$n_{AV} = \sqrt{(2n_{TE} + n_{TM})/3} \quad (1)$$

The in-plane refractive index of a thin PI film containing silica-modified TiO₂ nanoparticles was measured with a spectroscopic n&k analyzer (n&k Technology, Inc., model 1280) whose method is based on the Forouhi–Bloomer equation.

Calculations. The density functional theory (DFT) with the three-parameter Becke-style hybrid functional (B3LYP), which employs the Becke exchange and LYP correlation functions, was adopted for the calculation of the molecular polarizabilities in conjunction with the Gaussian basis sets. The 6–311G (d) basis set was used for geometry optimizations under no constraints, and 6–311++G (d,p) was used for calculating the linear polarizabilities.³⁴ All the calculations were performed using the software package of Gaussian-03 (Rev. C02 and D01).

Refractive indices of the pure PIs can be calculated using the Lorentz–Lorenz equation, which is given as follows

$$\frac{n^2 - 1}{n^2 + 2} = \frac{4\pi \rho N_A}{3 M_w} \alpha = \frac{4\pi}{3} \frac{\alpha}{V_{mol}} \quad (2)$$

where n is the refractive index; ρ , the density; N_A , Avogadro's number; M_w , the molecular weight; α , the linear molecular polarizability; and V_{mol} , the molecular volume. As shown in eq 2, the molecular volume or density of the material is required to calculate the refractive index. However, such parameters are generally difficult to predict because of the difficulty in estimating the states of molecular packing. In contrast, Van der Waals volumes (V_{vdw}) can be readily calculated from optimized geometries using Slonimskii's method,³⁵ in which the Van der Waals radii of atoms reported by Bondi are used.³⁶ The molecular packing constant K_p , defined in eq 3, can be used as a measure of molecular packing:

$$K_p = \frac{V_{vdw}}{V_{mol}} = \frac{\rho N_A}{M_w} V_{vdw} \quad (3)$$

The V_{mol} of a certain molecule is the summation of V_{vdw} and the intermolecular free spaces. For instance, in the case of dense molecular packing caused by intermolecular hydrogen bonds or charge-transfer interactions, the values of K_p increase because of a reduction in the intermolecular space. In this study, a typical K_p value of 0.60 was used for the prediction of the refractive indices.³⁷

The refractive index of the PI–TiO₂ nanocomposite was estimated by eq 4²⁸

$$n_{comp} = \varphi_p n_p + \varphi_{org} n_{org} = \frac{\rho_p n_{org} - \varpi_p (\rho_p n_{org} - \rho_{org} n_p)}{\rho_p - \varpi_p (\rho_p - \rho_{org})} \quad (4)$$

where n_{comp} , n_p , and n_{org} are the refractive indices of the nanocomposite, nanoparticle, and organic matrix, respectively. φ_p and φ_{org} are the volume fractions of the nanoparticles and organic matrix, respectively, and ϖ_p is the weight fraction of the nanoparticle.

Poly(amic acid) (PAA) synthesis. As a typical example, PAA-I_a was prepared according to the procedure described below. To a 100 mL three-necked round-bottom flask equipped with a high-power electromagnetic stirrer, nitrogen inlet, and cold-water bath was added 3SDA (2.1631 g, 5 mmol) and freshly distilled NMP (10.0 g). A clear diamine solution formed after stirring for 10 min under a nitrogen flow. Then, CBDA (0.9806 g, 5 mmol) was added immediately, followed by additional NMP (2.5 g) to adjust the solid content of the mixture to be 20% (wt %). The mixture was stirred at room temperature for 24 h to afford an almost colorless, highly viscous solution, which was diluted to 10 wt % by adding NMP (20 g). The mixture was stirred for an additional 1 h to obtain a homogeneous solution. After being purified by filtration through a 0.45 μm Teflon syringe filter (Toyo Roshi Kaisha, Ltd., Japan), the obtained poly(amic acid) (PAA) I_a solution was sealed and stored in a brown glass bottle filled with dry nitrogen in a refrigerator at –10 °C prior to use.

The other PAA solutions, including PAA-I_b (CBDA-APTT), PAA-II_a (CHDA-3SDA), and PAA-II_b (CHDA-APTT) were synthesized with a similar route.

PAA-II_a-TiO₂ Nanocomposite Preparation. A 100-mL three-necked flask equipped with a mechanical stirrer and a nitrogen inlet was charged with PAA-II_a solution (10 wt%, 5.5 g) and NMP (4.5 g). With stirring, the silica-modified TiO₂ nanoparticles (0.45 g) were added in one portion. The reaction mixture was stirred at room temperature for 12 h to afford a homogeneous solution with a total solid content of approximately 5 wt %. The solution was sealed in a brown glass bottle that was filled with dry nitrogen and stored in a refrigerator at –18 °C prior to use.

Polyimide Film Preparation. The stored PAA solution was warmed to room temperature and then spin-coated on a silicon wafer or quartz substrate (ϕ 50 mm, TKG Co., Ltd., Japan). The thickness was controlled by adjusting the spinning rate. The thickness of the specimens for the FT-IR and UV–vis measurements was controlled to be approximately 10 μm, and that of the specimens for thermal and mechanical property measurement was adjusted to 30–50 μm. PI films were obtained by thermally curing the PAA solution under nitrogen in an oven for 1 h each at 80, 150, 250, and 300 °C. Then, the PI films were obtained by immersing the substrate in warm

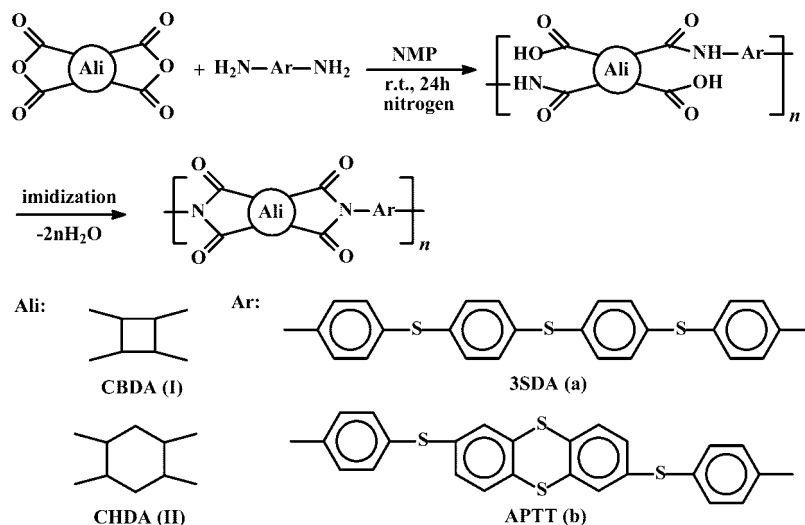
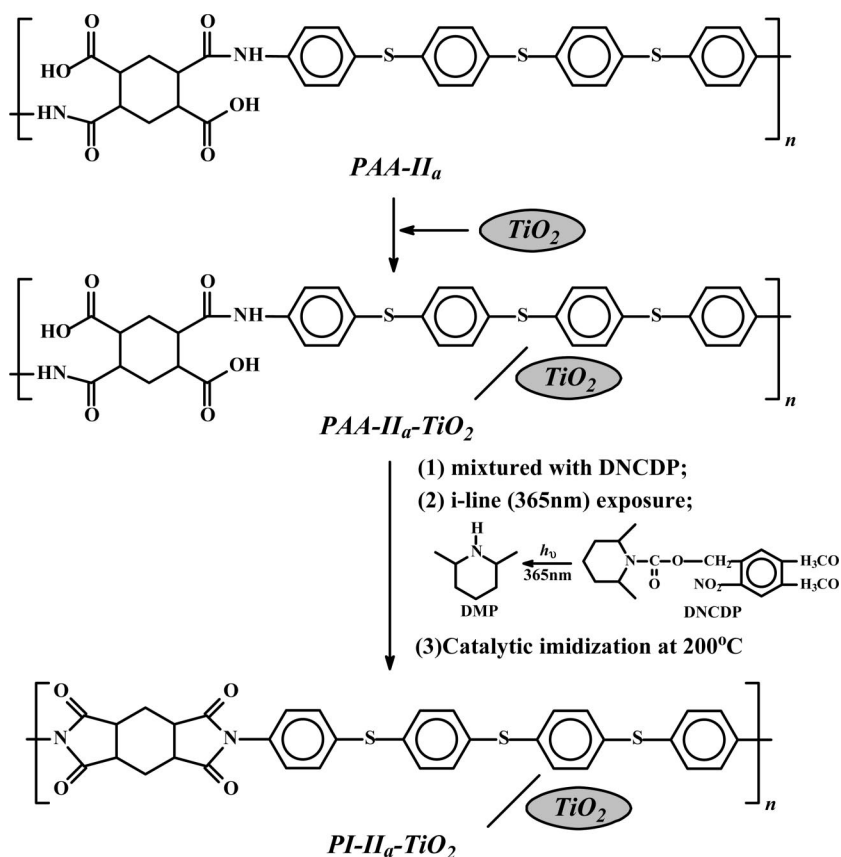
(34) Terui, Y.; Ando, S. *J. Polym. Sci., Part B: Polym. Phys.* **2004**, *42*, 2354.

(35) Slonimskii, G.; Askadskii, A.; Kitaigorodskii, A. *Polym. Sci. USSR* **1970**, *A12*, 556.

(36) Bondi, A. *J. Phys. Chem.* **1964**, *68*, 441.

(37) Terui, Y.; Ando, S. *J. Photopolym. Sci. Technol.* **2005**, *18*, 337.

Scheme 1. Synthesis of PIs

Scheme 2. Preparation of PI-IIa-TiO₂ Nanocomposite

water. After being dried in vacuum at 100 °C for 10 h, the PI films were characterized.

Photolithographic Evaluation of PAA-IIa-TiO₂ Nanohybrid.

A 1.0 μm thick photosensitive polymer film was prepared by adding DNCDP to PAA-II_a-TiO₂ in cyclohexanone, followed by spin-casting onto a silicone wafer and prebaking at 120 °C for 5 min. This film was exposed to 365 nm (i-line) light using a filtered superhigh-pressure mercury lamp and postbaked at 150 °C for 15 min. The exposed film was developed using a developer containing 2.38 wt% TMAH (aq.) at 25 °C for 60 s and then it was subsequently rinsed with distilled water. The characteristic sensitivity curve was obtained by plotting the normalized film thickness against the logarithmic exposure dose (units of mJ/cm²).

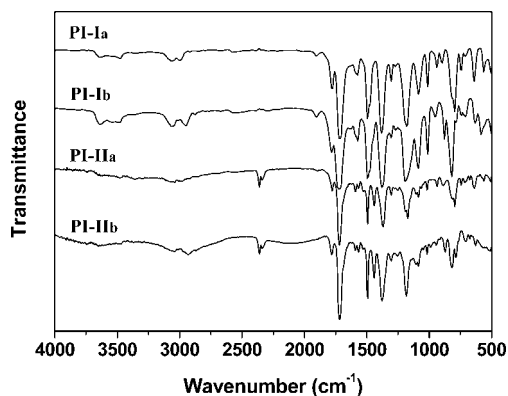
Results and Discussion

Polyimide Design and Synthesis. The aim of the present study is to develop optically transparent and photoimable high-*n* PI films. According to the Lorentz-Lorenz equation, a high molar refraction per unit molecular volume should result in a high refractive index. Thus, in the present work, to achieve a balance between high *n*, high transparency, and high *T_g*, two single-ring symmetric alicyclic dianhydrides, CBDA and CHDA, were selected to polymerize with the two sulfur-containing diamines, 3SDA and APTT, respectively. CHDA with a six-membered ring structure exhibits

Table 1. Polymerization and Film Properties of PIs

PAA	$[\eta]_{\text{inh}}^a$ (dL/g)	PI	film ^b	T_s^c (MPa)	E_b^c (%)	T_m^c (GPa)
PAA-I _a	1.03	PI-I _a	F&T, colorless	82	14	1.0
PAA-I _b	1.16	PI-I _b	F&T, pale brown	88	12	1.2
PAA-II _a	0.87	PI-II _a	F&T, colorless	98	16	1.7
PAA-II _b	0.98	PI-II _b	F&T, pale brown	96	14	1.6

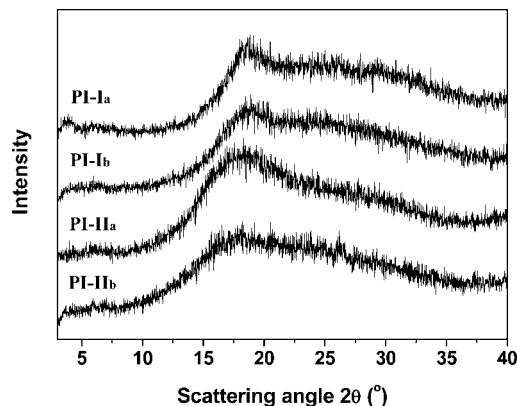
^a Measured with PAA at a concentration of 0.5g/dL in NMP solution at 30 °C. ^b Evaluated visually at a thickness of $\sim 10 \mu\text{m}$. F, flexible; T, tough. ^c T_s , tensile strength; E_b , elongation at break; T_m , tensile modulus.

**Figure 1.** FT-IR spectra of PI films.

a lower intramolecular stress and lower molecular packing density in comparison to CBDA. Thus, it is expected that the PIs derived from CHDA will exhibit a higher thermal stability, higher optical transparency, and at the same time, lower n values. On the other hand, the diamine 3SDA possesses a linear thioether linkage as opposed to the cyclic thioether (thianthrene) moiety in APTT. Thus, the PIs based on 3SDA should exhibit better optical transparency because of the reduced resonance length.

The synthetic procedure of the semialicyclic PIs is shown in Schemes 1 and 2. Highly viscous PAA solutions with inherent viscosities near or higher than 1.0 dL/g were obtained for all the polymerizations, indicating the high reactivity of the alicyclic dianhydrides. Flexible and tough PI films were obtained. The 3SDA-based PIs exhibit lighter colors than those of the APTT-based PIs, as shown in Table 1. For example, a PI-I_a film is colorless at a thickness of approximately $10 \mu\text{m}$, whereas PI-I_b shows a pale brown color at the same thickness. This phenomenon can be ascribed on the one hand to the semialicyclic molecular structures of the PIs, and on the other hand to the inherent light absorption characteristics of the thianthrene moiety in APTT associated with the conjugated structures.³⁸

The structures of the PIs are identified by their FT-IR spectra (Figure 1) in which the characteristic absorptions of the imide moiety located at ca. 1780 and 1720 cm^{-1} (asymmetric and symmetric stretching vibrations of the carbonyl group), and ca. 1387 cm^{-1} (vibration of C–N) as observed. The wide-angle X-ray diffraction (WAXD) curves, as shown in Figure 2, indicate that all the PIs are amorphous. The flexible thioether linkages and the nonplanar configuration of the thianthrene moiety are the main reasons for the absence of crystalline morphology.

**Figure 2.** WAXD patterns of PI films.

The mechanical properties, including tensile strength (T_s), elongation at break (E_b), and tensile modulus (T_m), of the PI films obtained as the average of five uniform samples are presented in Table 1. It is found that CHDA-based PIs (PI-II) exhibited better tensile properties than those derived from CBDA (PI-I). For instance, PI-II_a (CHDA-3SDA) has a T_s value of 98 MPa, E_b of 16%, and T_m of 1.7 GPa, which are higher than those of PI-I_a. The good tensile properties of the PI films reflect their flexible and tough nature, which are important for optical-field applications.

Thermal Properties. Long-term thermal and thermal-oxidative stability of the optical polymers are becoming more important because of the increasing heat-liberation problems caused by the increasing assembly densities and decreasing device sizes.³⁹ The deterioration of the performance of the optical devices associated with the thermal circumstances can be avoided by utilizing high-temperature-resistant polymers. Conventional PIs, after being elaborately modified, can meet most of the demands of advanced optical materials. In the present work, the thermal properties of the semialicyclic PIs are evaluated by TGA, DSC, and DMA.

The TGA curves measured in nitrogen and air are presented in Figure 3 and the results are listed in Table 2. It is obvious that all the PIs exhibit good thermal stabilities without significant weight loss up to approximately 400 °C , both in nitrogen and in air. The 5% weight loss temperatures ($T_{5\%}$) are higher than 420 °C in air and 430 °C in nitrogen. The residual weights at 600 °C (R_{w600}) are higher than 45% in air and 50% in nitrogen. It should be noticed that some PI samples showed higher $T_{5\%}$ values in air than those in nitrogen (Table 2). This phenomenon has also been observed for the other sulfur-containing polymers,⁴⁰ which might be attributed to the different thermal conductivities and densities of the gases.

The T_g values are in the range of 236.5 – 274.1 °C , based on the DSC measurement, as shown in Figure 4 and Table 2. The T_g was also measured by DMA for the CHDA-based PIs (PI-II_a and PI-II_b), as illustrated in Figure 5. The T_g determined as the peak temperature in the loss-modulus (E'') curves is 231.6 °C for PI-II_a and 247.7 °C for PI-II_b. In addition, PI-II_b shows a higher initial storage modulus (E')

(38) Wang, Y.; Chang, C. P.; Wu, Y. Z.; Tian, H. *Dyes Pigm.* **2001**, *51*, 127.

(39) Maier, G. *Prog. Polym. Sci.* **2001**, *26*, 3.

(40) Li, X. G.; Huang, M. R.; Bai, H.; Yang, Y. L. *J. Appl. Polym. Sci.* **2002**, *83*, 2053.

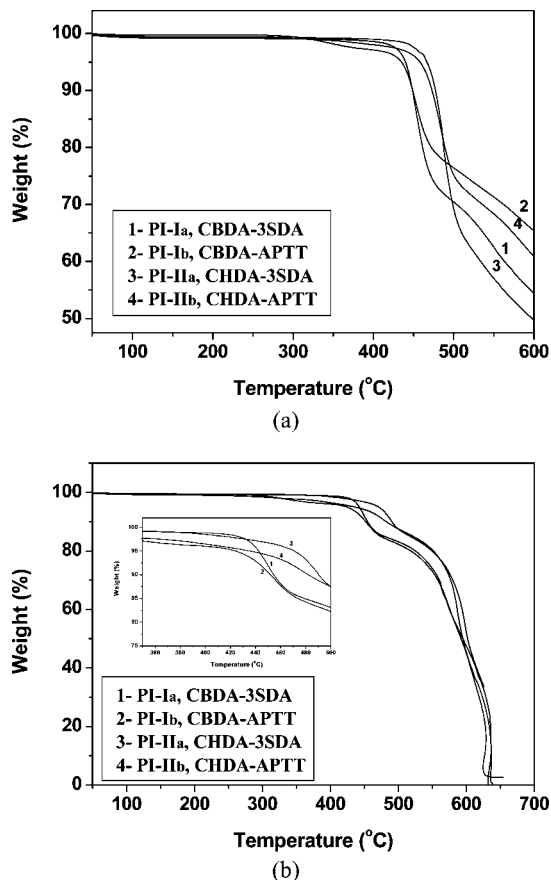


Figure 3. TGA curves of PI films in (a) nitrogen and (b) air (10 °C/min).

Table 2. Thermal Properties and Optical Dielectric Constants of PI Films^a

PI	T_g (°C)		$T_{5\%}$ (°C)		R_{w600} (%)		ϵ
	DSC	DMA	air	N ₂	air	N ₂	
PI-I _a	262.2		442.4	440.0	47.5	54.5	3.16
PI-I _b	274.1		424.0	434.9	45.0	65.4	3.23
PI-II _a	236.5	231.6	470.9	466.6	52.1	49.7	3.10
PI-II _b	261.8	247.7	435.6	458.2	45.2	60.9	3.17

^a T_g , glass-transition temperature; $T_{5\%}$, temperatures at 5% weight loss; R_{w600} , residual weight at 600 °C; ϵ , optical dielectric constant estimated from modified Maxwell's equation as $\epsilon = 1.10n_{av}^2$.

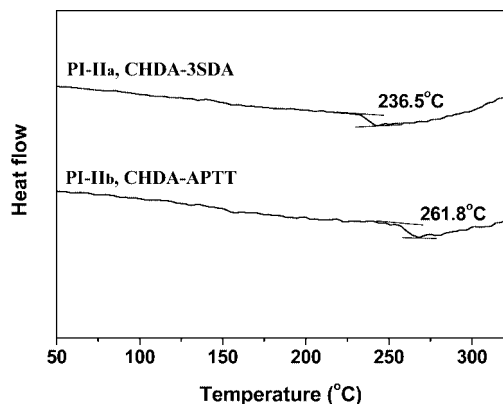


Figure 4. DSC curves of CHDA-based PIs (in nitrogen, 10 °C/min).

and E'' than those of PI-II_a because of the existence of a rigid thianthrene moiety in the former.

From the thermal data, certain trends can be easily identified. For example, the $T_{5\%}$ values of the PIs increase

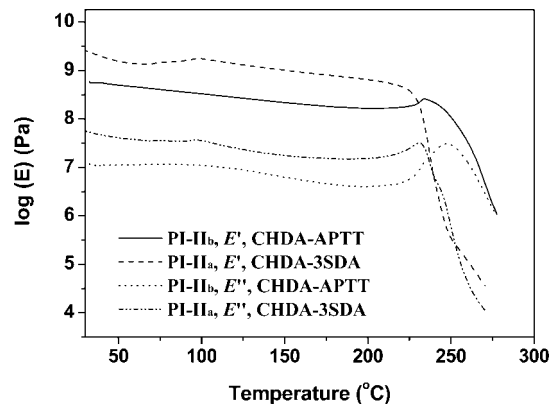


Figure 5. DMA curves of CHDA-based films (1 Hz, 2 °C/min).

in the order of PI-I_b < PI-II_b < PI-I_a < PI-II_a in air and PI-I_b < PI-I_a < PI-II_b < PI-II_a in nitrogen. Thus, the thermal and thermal-oxidative stabilities of the I series of PIs (CBDA series) are inferior to those of the II series of PIs (CHDA series), which can be ascribed to the lower internal stress at the cyclohexane structure in CHDA. At the same time, the PIs derived from 3SDA show better thermal properties than those from APTT. In fact, the decreased thermal stability of the thianthrene-based PIs or polyamides compared to their thioether analogs has been reported in the literature.⁴¹ The inferior thermal stability of the APTT-derived PIs may be ascribed to the structural stress caused by the nonplanar configuration of the cyclic thianthrene moiety. The T_g values of the PIs change with a reverse trend to the $T_{5\%}$. For example, the T_g values increase in the order of PI-II_a < PI-II_b \approx PI-I_a < PI-I_b, indicating that the PIs derived from 3SDA show lower T_g values than those from APTT. The high T_g values of thianthrene-based PIs are well-known in the literature⁴² and can be readily ascribed to the nonrotatable thianthrene moiety. Lee has clarified that the T_g behavior of semirigid PIs can be primarily explained as a function of the classical van der Waals forces and the chain flexibility of the repeating units.⁴³ In particular, they reported a function that expresses the T_g of PIs with “ether linkage density.” The present authors have reported that the energy barrier for the internal rotation of two phenyl rings in diphenyl sulfide is as low as 0.44 kJ/mol, which is significantly lower than that in diphenyl ether (0.79 kJ/mol).⁴⁴ Hence, the smaller numbers of diphenylsulfide linkages (two) in APTT than those in 3SDA (three) lead to the increase in T_g in APTT-derived PIs.

Optical Properties. The present semialicyclic PI films exhibit good transparency above 400 nm, as shown in the UV–vis spectra in Figure 6 and the data provided in Table 3. The PI films show the cutoff wavelengths at about 340 nm, which are ca. 50 nm shorter than that of the wholly aromatic PI derived from 3,3',4,4'-biphenyltetracarboxylic dianhydride (sBPDA) and 3SDA (depicted as a reference).³⁰ The transmittances of the PI films at 365 nm are greater than

(41) Niume, K.; Hirohata, R.; Toda, F.; Hasagawa, M.; Iwakura, Y. *Polymer* **1981**, 22, 649.

(42) Johnson, R. A.; Mathias, L. J. *Macromolecules* **1995**, 28, 79.

(43) Lee, C. J. *J. Macromol. Sci., Rev. Macromol. Chem. Phys.* **1989**, C29, 431.

(44) Aimi, K.; Fujiwara, T.; Ando, S. *J. Mol. Struct.* **2001**, 602–603, 405.

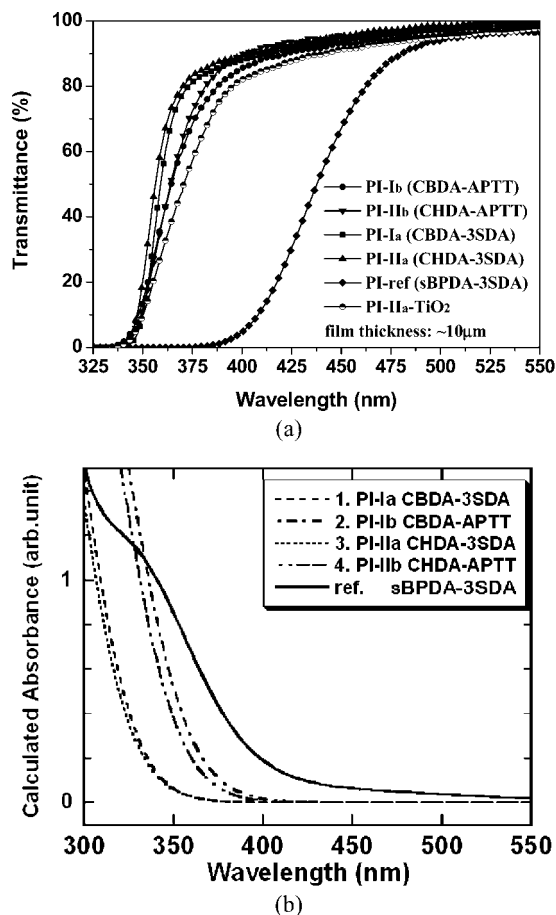


Figure 6. (a) Experimental and (b) calculated UV-vis spectra of PI films.

50% in comparison to the opaque nature of sBPDA-3SDA at the same wavelength. The good transmittances of the present PI films at 365 nm facilitate the formation of fine patterns using the i-line photolithography technique. The increased optical transparency can be mainly attributed to the reduction in inter and intramolecular charge-transfer (CT) interactions and the reduction in extended conjugation along the polyimide backbone. In addition, the 3SDA-based PIs (PI-I_a and PI-II_a) show a better optical transparency than that of APTT-based ones because of the inherent light absorption characteristics of the thianthrene moiety in APTT.³⁸ The hybrid of nano TiO₂ particles into the PI-II_a sacrificed the optical transparency of the film to some extent. For example, the 10 μm thickness PI-II_a-TiO₂ films exhibit the transmittance of 40% at 365 nm, which is 33% lower than that of the pure PI-II_a film.

The experimental and calculated refractive indices are depicted in Table 3. As expected, the introduction of an alicyclic moiety decreases the RI values in comparison with the wholly aromatic PIs due to the decrease in the aromatic components. For example, the n_{av} values of sBPDA-3SDA and sBPDA-APTT are 1.7327 and 1.7547 at 632.8 nm, respectively,^{31,32} which are higher than the maximum RI value obtained for PI-I_b (1.7130). Moreover, the PIs derived from APTT (PI-I_b and PI-II_b) exhibit higher n_{av} values than those from 3SDA (PI-I_a and PI-II_a) because of the higher sulfur contents of the former.

The values of the in-plane/out-of-plane birefringence (Δn), estimated as a difference between n_{TE} and n_{TM} , are also

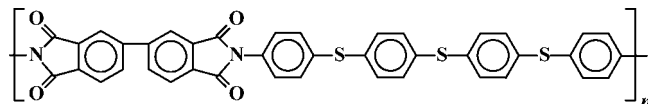
provided in Table 3. The PIs derived from CBDA (PI-I_a and PI-I_b) exhibit significantly larger Δn than those from CHDA (PI-II_a and PI-II_b). This is attributable to the more planar structure of the CBDA moiety. It should be noted that the Δn values of the PIs derived from CBDA are larger than that of the completely aromatic reference PI (sBPDA-3SDA, see Table 3), which indicates that the polymer chains in the former are more densely packed and oriented in the film plane. The dense molecular packing is well-supported by the fact that the experimental RI values for PI-I_a and PI-I_b are significantly higher than the calculated RI values (Table 3). The packing coefficients (K_p) estimated from the experimental n values, calculated van der Waals volumes, and molecular polarizabilities³⁰ are 0.629, 0.602, 0.545, 0.548, and 0.602 for PI-I_a, I_b, II_a, II_b, and sBPDA-3SDA, respectively. In addition, the estimated K_p value for sBPDA-APTT is 0.590.³² These values clearly indicate that CBDA induces more densely packed molecular chains of PIs than those of CHDA and sBPDA, which is the main cause of the higher n_{av} values and the higher Δn values of PI-I_a and PI-I_b. On the other hand, CHDA induces loose molecular packing, as evidenced by the significantly smaller K_p values for PI-II_a and PI-II_b. This should also be reflected in the better transparency of CHDA-derived PIs in the UV region in comparison to the CBDA-derived PIs.

As expected, the PI-II_a film showed the best optical transparency, high refractive index (1.6799), and lowest birefringence (0.0048); thus, it was adopted to be combined with titania nanoparticles. The TiO₂ nanoparticles used in this work are modified by the silica. As a nontoxic, thermal, and environmentally stable nanoparticle, TiO₂ is widely used in many high-tech fields. However, the surface chemistry of TiO₂ nanoparticle is rather complex and quite dependent on the synthetic method and on the crystalline state.⁴⁵ Thus, in some special applications, especially in optical areas, the surface of the TiO₂ nanoparticles is often functionalized by grafting substituents such as silica. This modification often changes the physical and chemical properties of the nanoparticles, such as a decrease in density and refractive index or an increase in the hydrophobic nature of the surface. For example, the anatase TiO₂ nanoparticles usually have a refractive index of 2.45 at 589 nm; however, after modification with silica, the value decreases to 2.00. The silica-modified TiO₂ nanoparticles showed good affinity with a PAA-II_a solution in the proportion of PAA:TiO₂ = 55:45 (w/w). A homogeneous mixture was easily achieved using a mechanical stirrer. The nanocomposite film exhibited good uniformity, as evidenced by the SEM investigation shown in Figure 7. The homogeneous and transparent nanocomposite film had a refractive index of 1.8100 at 632.8 nm, which confirmed our molecular design and achieved the initial target ($n > 1.80$). The n value of the PI-II-TiO₂ nanocomposite could also be approximately estimated from eq 4 with the parameters of $\rho_p = 3.11 \text{ g/cm}^3$, $n_{p,589\text{nm}} = 2.00$, and $n_{org,633\text{nm}} = 1.68$. The density of the PI film is often in the range of 1.3–1.5 g/cm³, depending on the structure of

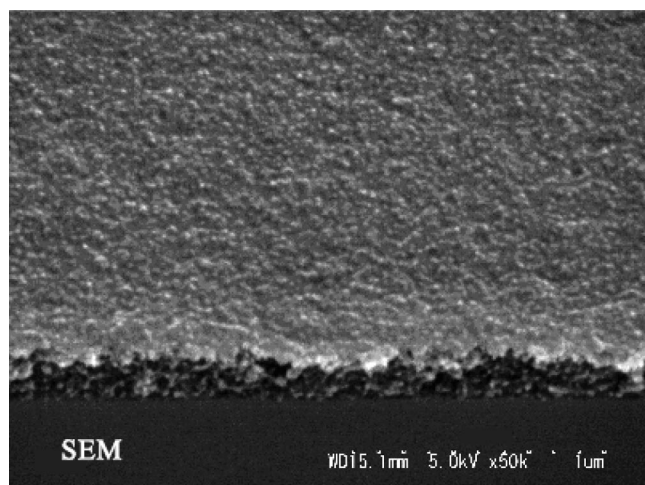
(45) Baraton, M.; Merhari, L. *J. Eur. Ceram. Soc.* **2004**, *24*, 1399.

Table 3. Optical Properties of PI Films

PI	S_c^a (wt%)	$\lambda_{\text{cutoff}}^b$ (nm)	T_{365}^c (%)	d^d (μm)	refractive index at 632.8 nm ^e				
					n_{TE}	n_{TM}	Δn	n_{av}	n_{cal}
PI-I _a	16.2	344	68.8	4.9	1.7018	1.6815	0.0203	1.6951	1.6557
PI-I _b	20.6	340	51.6	7.2	1.7203	1.6983	0.0220	1.7130	1.7096
PI-II _a	15.5	341	73.0	3.0	1.6815	1.6767	0.0048	1.6799	1.6409
PI-II _b	19.7	342	52.6	18.6	1.6994	1.6935	0.0059	1.6974	1.6912
PI _{ref} ^g	13.9	394	0.0	8.9	1.7393	1.7270	0.0123	1.7352	1.7327
PI-II _a -TiO ₂	—	343	40.0	0.16				1.810 ^f	1.780

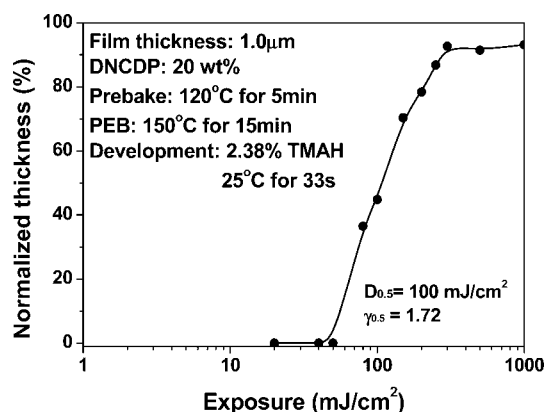
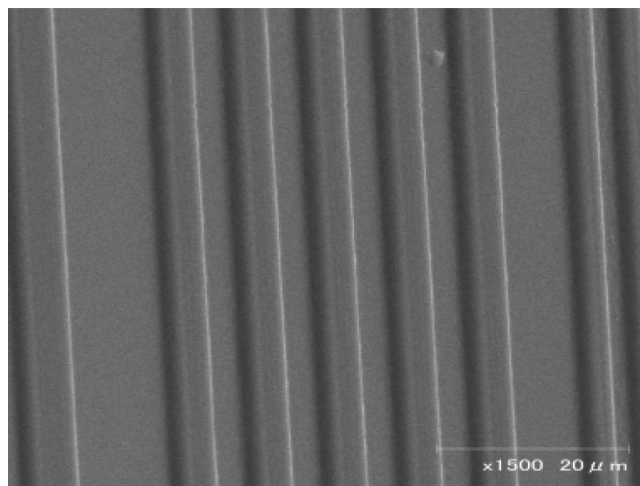


^a Sulfur content. ^b Cut-off wavelength. ^c Transmittance at 365 nm. ^d Film thickness. ^e See measurements. ^f Obtained by spectroscopic n&k analyzer at 632.8 nm. ^g sBPDA-3SDA with the above structure.³⁰

Figure 7. SEM pictures of PI-II_a-TiO₂ (55:45 w/w) nanocomposite film.

the PIs.⁴⁶ In the present research, considering the high packing coefficient of the PI-II_a, the density was supposed to be $\rho_{\text{org}} = 1.45 \text{ g/cm}^3$. Thus, the estimated n_{comp} value is around 1.78, which is lower than that of the experimental value (1.81). The difference might be ascribed to the numerical errors in the values of $n_{\text{p},589\text{nm}}$ and ρ_{org} .

Lithographic Evaluation for PAA-II_a-TiO₂ Nano-hybrid. In a previous paper, we reported a negative-type photosensitive polyimide (PSPI) based on a PAA and photobase generator.⁴⁷ This resist system was applied to the pattern formation for the present PAA-II_a-TiO₂ nanocomposite. A photosensitive polymer consisting of PAA-II_a-TiO₂ (80 wt %) and DNCDP (20 wt %) as the photobase generator was formulated. The photosensitivity curve of the nanocomposite film at a thickness of 1.0 μm is shown in Figure 8. The photoresist system showed a sensitivity ($D_{0.5}$) of 110 mJ/cm^2 and a contrast ($\gamma_{0.5}$) of 1.72 with i-line (365 nm). Figure 9 shows a characteristic SEM image of a contact-printed pattern obtained with a 1.0 μm photoresist film exposed with an i-line of 500 mJ/cm^2 , postbaked at 150 °C for 15 min, and developed with 2.38 wt % TMAH aqueous solution at 25 °C for 60 s. A clear negative-tone image with a 4 μm line and space resolutions was obtained.

Figure 8. Photosensitivity curve of PAA-II_a-TiO₂-DNCDP PSPI system.Figure 9. SEM image of negative PSPI pattern (film thickness: 1.0 μm).

Conclusions

Highly transparent and highly refractive semialicyclic PIs were synthesized and characterized. The relationships between the structures and the physical properties of the semialicyclic PIs were investigated and established. The introduction of alicyclic dianhydride moieties increased the optical transparency and T_g values, whereas it decreased the thermal stability and refractive indices of the polymers to some extent. The PIs derived from CBDA demonstrated higher refractive indices and larger in-plane/out-of-plane birefringence than those from CHDA; this phenomenon

(46) Xu, Y. X.; Chen, C. X.; Zhang, P. X.; Sun, B. H.; Li, J. D. *J. Appl. Polym. Sci.* **2007**, *103*, 998.

(47) Fukukawa, K.; Shibasaki, Y.; Ueda, M. *Polym. Adv. Technol.* **2006**, *17*, 131.

originates from the dense molecular packing in the former PIs because of the more planar dianhydride structure. The refractive indices of the PIs synthesized in this study were slightly lower than those of wholly aromatic PIs, but they were sufficient enough to meet the requirements of optical polymers. The good transmittances of the semialicyclic PI films at 365 nm facilitated the formation of fine patterns by the i-line photolithography technique. The refractive index was well-remedied by combining with TiO₂ nanoparticles. The inherent high refractive index of the PI-II_a matrix made it possible to achieve a refractive index higher than 1.80 with

a relatively small TiO₂ loading (45 wt %). Furthermore, a negative-type PSPI was formulated from PAA-II_a-TiO₂ and DNCDP. The photosensitivity and contrast ($\gamma_{0.5}$) of the hybrid PI-II_a-TiO₂ composite (80 wt %) and DNCDP (20 wt %) were 100 mJ/cm² and 1.72, respectively. This resist system produced a clear negative-tone image with 4 μ m line and space resolutions. The photoresist system based on PAA-II_a-TiO₂ and DNCDP with a refractive index of 1.81 produced a good pattern profile and is a good candidate for CIS fabrication.

CM071430S